International Journal of Nanomedicine

Dovepress
open access to scientific and medical research

Open Access Full Text Article

ORIGINAL RESEARCH

# Preclinical evaluation of sorafenib-eluting stent for suppression of human cholangiocarcinoma cells



This article was published in the following Dove Press journal:
International Journal of Nanomedicine
29 April 2013
Number of times this article has been viewed

Do Hyung Kim[1,2,*]
Young-Il Jeong[1,*]
Chung-Wook Chung[1]
Cy Hyun Kim[1,2]
Tae Won Kwak[1]
Hye Myeong Lee[1]
Dae Hwan Kang[1,2]

[1]National Research and Development Center for Hepatobiliary Cancer, Pusan National University Yangsan Hospital, [2]School of Medicine, Pusan National University, Yangsan, Gyeongsangnam-do, South Korea

*These authors equally contributed to this work.

**Background:** Cholangiocarcinoma is a malignant tumor arising from the epithelium of the bile ducts. In this study, we prepared sorafenib-loaded biliary stents for potential application as drug-delivery systems for localized treatment of extrahepatic cholangiocarcinoma.

**Methods:** A sorafenib-coated metal stent was prepared using an electrospray system with the aid of poly(ε-caprolactone) (PCL), and then its anticancer activity was investigated using human cholangiocellular carcinoma (HuCC)-T1 cells in vitro and a mouse tumor xenograft model in vivo. Anticancer activity of sorafenib against HuCC-T1 cells was evaluated by the proliferation test, matrix metalloproteinase (MMP) activity, cancer cell invasion, and angiogenesis assay in vitro and in vivo.

**Results:** The drug-release study showed that the increased drug content on the PCL film induced a faster drug-release rate. The growth of cancer cells on the sorafenib-loaded PCL film surfaces decreased in a dose-dependent manner. MMP-2 expression of HuCC-T1 cells gradually decreased according to sorafenib concentration. Furthermore, cancer cell invasion and tube formation of human umbilical vein endothelial cells significantly decreased at sorafenib concentrations higher than 10 mM. In the mouse tumor xenograft model with HuCC-T1 cells, sorafenib-eluting PCL films significantly inhibited the growth of tumor mass and induced apoptosis of tumor cells. Various molecular signals, such as B-cell lymphoma (Bcl)-2, Bcl-2-associated death promoter, Bcl-x, caspase-3, cleaved caspase-3, Fas, signal transducer and activator of transcription 5, extracellular signal-regulated kinases, MMP-9 and pan-janus kinase/stress-activated protein kinase 1, indicated that apoptosis, inhibition of growth and invasion was cleared on sorafenib-eluting PCL films.

**Conclusion:** These sorafenib-loaded PCL films are effective in inhibiting angiogenesis, proliferation and invasion of cancer cells. We suggest that sorafenib-loaded PCL film is a promising candidate for the local treatment of cholangiocarcinoma.

**Keywords:** sorafenib, polycaprolactone, biliary stent, human cholangiocarcinoma cells, angiogenesis

Correspondence: Dae Hwan Kang
National Research and Development Center for Hepatobiliary Cancer, Research Institute for Convergence of Biomedical Science and Technology, Pusan National University Yangsan Hospital, Beomeo-ri, Mulgeum-eup, Yangsan, Gyeongsangnam-do 626-770, South Korea
Tel +82 55 360 3870
Fax +82 55 360 3879
Email sulsulpul@yahoo.co.kr

## Introduction

Cholangiocarcinoma is a malignant tumor arising from the epithelium of the bile ducts, to which bile is drained from the liver to be emptied into the small intestine.[1] Cholangiocarcinoma characterized by early vascular invasion and metastasis is anatomically subdivided into intrahepatic and extrahepatic types.[2,3] The medical treatment options for cholangiocarcinoma are radiation, chemotherapy, stent placement, and surgical resection. In current clinical trials for chemotherapy, gemcitabine is known to have efficacy for the treatment of advanced gallbladder cancer or cholangiocarcinoma.[4] Furthermore, clinical gains in chemotherapeutic approaches were also

submit your manuscript | www.dovepress.com
Dovepress
http://dx.doi.org/10.2147/IJN.S43508

reported with combinations of anticancer drugs.[4–9] Among them, clinical trials with a combination of gemcitabine plus cisplatin were reported to have significant survival advantage compared to gemcitabine alone.[7–9] However, systemic chemotherapy and radiation therapy for cholangiocarcinoma is not sufficiently effective. In current clinical treatment for cholangiocarcinoma, stent displacement is believed to be a unique candidate for the enhancement of patient survivability.[10] Metal stents enable bile drainage when tumors block the bile duct. After placement of metal stents, occlusion of the stent can occur by in-stent proliferation of cells, resulting in deposition of biliary sludge and progression of disease. Those processes cause a risk of sepsis and recurrent biliary obstruction.[3] The current stent allows only mechanical palliation of the obstructed gastrointestinal tract without providing antitumor effects.[11] Furthermore, bile duct cancer is characterized by relatively small size with local rather than systemic metastasis. Therefore, local treatment with devices such as drug-eluting stents (DESs) is a promising therapeutic candidate.

Sorafenib is known to inhibit tumor cell proliferation and vascularization through activation of the receptor for tyrosine kinase, which in turn signals the Ras/Raf/ mitogen-activated protein kinase kinase (MEK)/extracellular-signal-regulated kinase (ERK) cascade pathway.[12] Sorafenib is an effective chemotherapeutic agent against various tumor types, including cholangiocarcinoma,[13] and is known to inhibit proliferation, angiogenesis, and invasion of tumor cells;[13–15] positive case studies have been reported against cholangiocarcinoma.[13–16] Furthermore, anticancer activity of sorafenib against cholangiocarcinoma cells was also reported in in vitro cell culture and in in vivo tumor xenograft models.[17,18] Based on these studies, local treatment of sorafenib can be considered an attractive option for advanced chemotherapy of cholangiocarcinoma.

In this study, we prepared a sorafenib-coated DES with the aid of biodegradable poly(ε-caprolactone) (PCL) to test its anticancer activity against cholangiocarcinoma cells. We determined the optimal conditions of sorafenib-coated DESs using appropriate organic solvents, drug/polymer ratios, and drug-release media. Furthermore, the anticancer activity of sorafenib itself and sorafenib-coated DESs against human cholangiocellular carcinoma (HuCC)-T1 cells was investigated in vitro/in vivo using growth inhibition, matrix metalloproteinase expression, Matrigel assay for cancer cell invasiveness, and angiogenesis assays.

# Materials and methods

## Materials

PCL (number average molecular weight 70,000–90,000) was purchased from Sigma-Aldrich (St Louis, MO, USA). Sorafenib was purchased from LC Laboratories (Woburn, MA, USA). All solvents, ie, dichloromethane, tetrahydrofuran, and chloroform, purchased from Honeywell (Morristown, NJ, USA) were of extra-pure grade, while other solvents used were of high-performance liquid chromatography grade.

## Stent-coating method

A sorafenib-coated stent was prepared with bio-spray-coating equipment (EBS ES-Biocoater; Nano NC, Seoul, South Korea). The electrospray consisted of a high-voltage power supply, syringe pump, X-Y robotic system, and Drum-roll collector. One hundred milligrams of PCL was dissolved in 10 mL of dichloromethane. To this solution, sorafenib dissolved in dimethyl sulfoxide (DMSO; 200 mg/mL) was added, and a final concentration of sorafenib was adjusted to 2%–10% (w/w) versus PCL. Ten milliliters of this solution (100 mg PCL and 10 mg sorafenib) was introduced into a syringe and then sprayed onto a rolling collector (diameter 1 cm, length 10 cm, rolling speed 800 rpm, voltage 10 kV) at a speed of 100 mL/minute. Next, the sorafenib-coated stent was dried for 3 hours and then carefully isolated from the collector and weighed.

The morphology of the polymer surface was examined using a field-emission scanning electron microscope (S-4800; Hitachi, Tokyo, Japan) at 25 kV.

## In vitro release studies

The sorafenib-coated stent prepared by the method described above was placed in 15 mL conical tubes with 10 mL of Roswell Park Memorial Institute (RPMI) 1640 medium supplemented with 10% fetal bovine serum (FBS). This tube was placed in an orbital shaker at 100 rpm at 37°C. At specific time intervals, the whole media was taken to measure the released drug and was replaced with fresh media every day. Drug concentration was determined by high-performance liquid chromatography analysis. Furthermore, sorafenib-released media was used to test whether sorafenib maintained its biological activity during the stent-coating process and drug-release experiment. At 1, 5, 10, 15, 20, and 30 days of the drug-release experiment, the collected media were used to test anticancer activity.

## Polymer-degradation tests

The unloaded PCL film or sorafenib-loaded PCL film (10% [w/w] sorafenib) was immersed in 100 mL of

phosphate-buffered saline (PBS; 0.01 M, pH 7.4), artificial bile solution (15 mM sodium phosphate buffer, pH 7.4, 62 mM NaCl, 2.5% glucose, 6.6 mM sodium taurocholate, 0.6 mM phosphatidylcholine), and 0.01 N NaOH (pH 12). The degradation test was carried out at 100 rpm at 37°C. The media was changed every week for 3 months. At predetermined time intervals, the films were rinsed with distilled water and dried to analyze weight loss of the polymer surface:

$$\text{Weight loss of PCL film}$$
$$W_L = (W_i - W_d)/W_i \times 100\%$$

where $W_i$ is the initial weight of the film and $W_d$ is the weight of the film after the degradation time interval.

## Cell culture

HuCC-T1 cells were purchased from the Health Science Research Resources Bank (Osaka, Japan). To measure growth inhibition of cancer cells, $3 \times 10^3$ cells were seeded in 96-well plates and incubated overnight in an incubator with 5% $CO_2$ at 37°C. Following incubation, sorafenib or sorafenib-released media (sorafenib-released media from polymer described above) were added to this plate. Control was 0.1% v/v DMSO. The cells were incubated for an additional 32 hours. Subsequently, 25 µL of MTT (3-[4,5-dimethylthiazol-2-yl]-2,5-diphenyltetrazolium bromide; 3 mg/mL) was added to each well. After 4 hours, 100 µL of sodium dodecyl sulfate (SDS)-hydrochloric acid (HCl) solution (SDS 10% w/v, 0.01 M HCl) was added to each well, and after 12 hours absorbance was measured at 570 nm (Infinite M200 Pro microplate reader; Tecan, Männedorf, Switzerland). Viable cells were expressed as a percentage of control. Results were calculated as the means ± standard deviation of three different experiments.

## Gelatin zymography

Gelatin zymography was performed as described previously. A total of $5 \times 10^5$ HuCC-T1 cells seeded in six-well culture plates were cultured with serum-free media. The cells were treated with sorafenib or sorafenib-released media and then incubated for an additional 32 hours. The conditioned media were then collected and centrifuged to remove cell debris. Concentrated proteins (50 mg) were mixed with nonreducing sample buffer (0.5 M Tris-HCl pH 6.8, 4% SDS, 20% glycerol, 0.1% bromophenol blue) at a 1:1 ratio and electrophoresed on 8% SDS-polyacrylamide gels (SDS-PAGE) containing 2 mg/mL gelatin (Bio Basic, Markham, ON, Canada) under nonreducing conditions. After electrophoresis, the gel was washed three times for 30 minutes at room temperature in a 2.5% (v/v) Triton X-100 solution to remove SDS and then incubated in zymogram development solution (50 mM Tris-HCl pH 7.5, 5 mM $CaCl_2$, 200 mM NaCl) for 24 hours at 37°C. The gel was stained with Coomassie Brillant Blue R-250 (0.2% Coomassie Brillant Blue R-250, 20% methanol and 10% acetic acid in $H_2O$), then destained (20% methanol and 10% acetic acid in $H_2O$).

## Flow cytometry analysis

Fluorescein isothiocyanate-annexin V and propidium iodide (PI) were used to identify apoptosis and necrosis of HuCC-T1 cells. Cells were treated with various concentrations of sorafenib or sorafenib-released media for 24 hours. Following treatment, the cells were collected and washed with PBS. The collected pellets were resuspended with binding buffer (10 mM 4-[2-hydroxyethyl]-1-piperazineethanesulfonic acid pH 7.4, 150 mM NaCl, 5 mM KCl, 1 mM $MgCl_2$, 1.8 mM $CaCl_2$) containing fluorescein isothiocyanate-annexin V (1 µg/mL) and further incubated for 30 minutes. Ten minutes prior to the termination of incubation, PI (10 µg/mL) was added to stain necrotic cells under dark conditions. The cells were immediately analyzed using a FACScan flow cytometer (BD Biosciences, San Jose, CA, USA).

## Matrigel invasion assay

Invasion assays were performed using a transwell chamber.[19] A polyethylene terephthalate (PETE) membrane (pore size 8 µm; BD Biosciences) was coated with Matrigel (BD Biosciences) diluted in serum-free RPMI 1640 medium (RPMI:Matrigel = 4:1) at 4°C. A total of $2 \times 10^4$ HuCC-T1 cells in 100 µL of serum-free media were seeded in the upper compartment of transwells and allowed to invade the PETE membrane in the lower chamber for 2 days. The lower chamber was filled with RPMI medium supplemented with 10% FBS with various concentrations of sorafenib and sorafenib-released media. After that, noninvaded cells on the upper surface of the membrane were removed, and the invaded cells on the lower surface of the membrane were stained with the Hemacolor rapid staining kit (Merck KGaA, Darmstadt, Germany). The invaded cells were observed with an optical microscope (Micros, St Veit/Glan, Austria). The number of cells in four randomly selected microscopic fields per membrane was counted.

## Angiogenesis assay

An angiogenesis assay was performed as reported by Okabe et al.[20] When HuCC-T1 cells filled the dishes to 70%–

80% confluence, the medium was replaced with serum-free RPMI 1640. The cells were then treated with various concentrations of sorafenib or sorafenib-released media for 32 hours. After that, the media were centrifuged at 1000 rpm for 5 minutes, and the collected supernatant was used as conditioned media. The protein content of the conditioned media was determined by a BCA Protein Assay Kit (Thermo Fisher Scientific, Waltham, MA, USA), and aliquots were stored at −80°C until use. Human umbilical vein endothelial cells (HUVECs; $1 \times 10^4$ cells/well) were suspended in a mixture of conditioned media/EGM-2 medium (100 µL/100 µL) with 0.5% FBS and seeded on 50 µL of Matrigel in 96-well plates. These plates were incubated for 12 hours, and then the morphology of the cells in each well was examined. The total capillary tube length and branching points were examined in three random view-fields per well, and average values were calculated.

## Wound-healing assay

A wound-healing assay of HuCC-T1 cells was performed using a wound-healing assay kit containing Ibidi (Planegg, Germany) culture inserts. Aliquots containing $5 \times 10^5$ cells in RPMI 1640 media were seeded on six-well plates, and the cells were exposed to sorafenib or sorafenib-released media at 37°C and 5% $CO_2$ for 24 hours. The cells were washed twice with PBS and harvested. Next, $5 \times 10^4$ cells in serum-free media were seeded into culture inserts following incubation for 24 hours. The zone of wound healing and migrated cells was observed using light microscopy.

## Effect of sorafenib-coated stent on the growth of HuCC-T1 cells

The films cast in glass plates with a diameter of 3 cm were sterilized under ultraviolet radiation. A total of $5 \times 10^5$

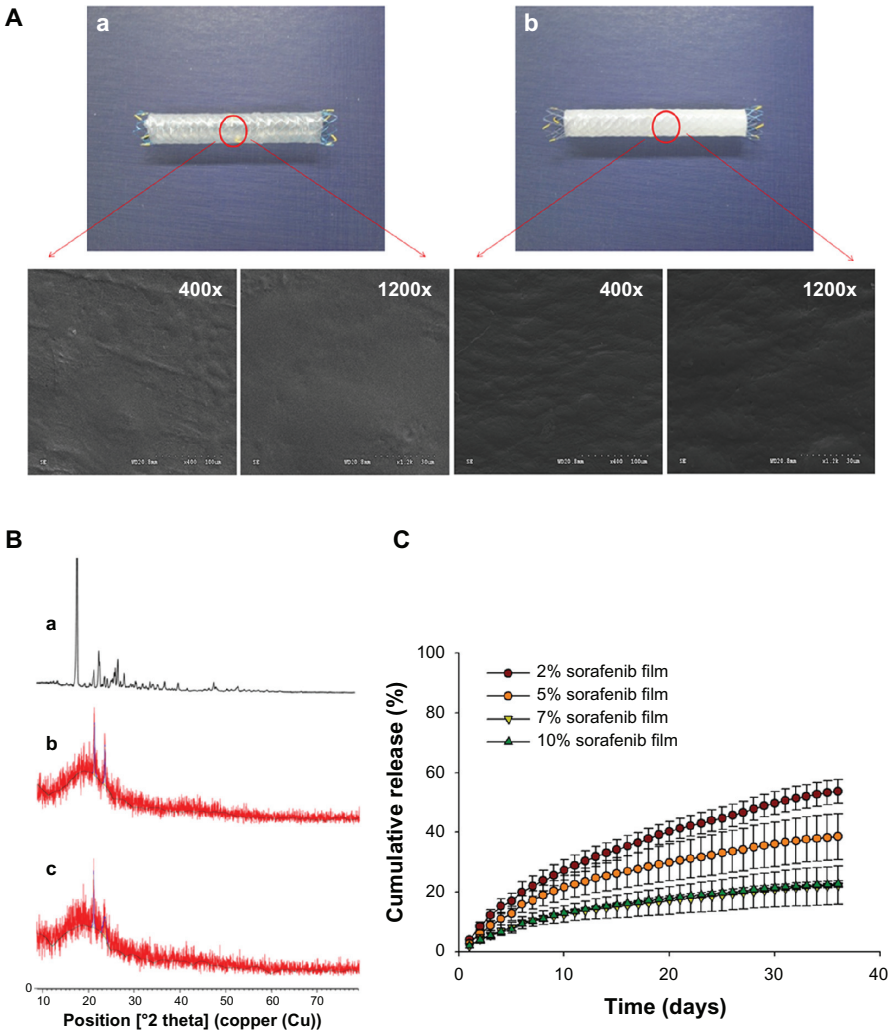


**Figure 1** (**A**) Morphological observation of sorafenib-loaded stent: field-emission scanning electron microscopy images of unloaded stent (**a**) and sorafenib-loaded stent (**b**). Poly(ε-caprolactone) as a coating polymer was dissolved in dichloromethane. After that, sorafenib in a small amount of dimethyl sulfoxide was added to this solution and spray-dried onto a bare metal stent. (**B**) X-ray diffraction spectra of sorafenib powder (**a**), sorafinib film (**b**), and unloaded film (**c**). (**C**) The effect of drug contents on the sorafenib release from the stent.

HuCC-T1 cells were seeded on the films and cultured for 32 hours. The nuclei of cancer cells were stained with eosin using the Hemacolor rapid staining kit according to the manufacturer's protocol.

## In vivo animal tumor xenograft study

HuCC-T1 cells ($1 \times 10^7$ cells) in a total volume of 100 µL were subcutaneously injected into the back of male nude mice (5 weeks old and 20–25 g in weight, Orient, Seongnam, South Korea). When the tumor diameter reached about 6 mm, a sorafenib-eluting PCL film was surgically implanted under the tumor. Treatment dose was adjusted to 200 µg of sorafenib (10 mg/kg). A total of 30 mice were divided into three groups, as follows: (1) nonimplanted, (2) empty PCL film-implanted, and (3) sorafenib-loaded film-implanted. Body weight and tumor volume were measured twice weekly, starting on the first day of treatment. Two perpendicular diameters of the tumor were measured, and tumor volume was calculated using the formula $V = (a \times [b]^2)/2$, with $a$ dUDT being the largest and $b$ being the smallest diameter.

Animal study was carried out according to the guidelines of the Animal Treatment and Research Council of Pusan National University.

## Histological analysis

Tumors were removed 30 days after film implantation, fixed in 4% formamide, paraffin-embedded, and sliced for hematoxylin and eosin staining or for terminal deoxynucleotidyl transferase dUDT nick-end-labeling (TUNEL) assay.

## Immunohistochemistry

Immunohistochemical staining of paraffin sections of the tumors was done with matrix metalloproteinase (MMP)-9 antibody at a dilution of 1:100, with caspase-3 antibody at a dilution of 1:200, with cleaved caspase-3 antibody (cell-signaling technology) at a dilution of 1:1600, and with B-cell lymphoma (Bcl)-2, Bcl-2-associated death promoter, Bcl-x, signal transducer and activator of transcription (STAT)-5, pan-janus kinase/stress-activated protein kinase 1, ERK1, and Fas/CD95/APO-1 (BD Biosciences) at a dilution of 1:100. Staining was done using an Envision kit (Life Technologies, Carlsbad, CA, USA) according to the manufacturer's protocol.

# Results

## Characteristics of sorafenib-incorporated PCL films

Sorafenib-loaded and unloaded PCL film-covered stents were prepared by the electrospray method shown in Figure 1.

**Table 1** Characterization of sorafenib-coated stent

| Polymer/drug (mg/mg) | Coating efficiency | Coating thickness (mm) | Sorafenib concentration per unit area (mg/cm$^2$) |
|---|---|---|---|
| 100/0 | 61.39 ± 7.16 | 23.33 ± 1.37 | |
| 100/2 | 61.49 ± 8.12 | 24.33 ± 3.01 | 45.28 ± 8.25 |
| 100/5 | 61.55 ± 10.53 | 24.67 ± 1.37 | 113.19 ± 20.63 |
| 100/7 | 65.30 ± 6.75 | 25.17 ± 1.94 | 158.47 ± 28.88 |
| 100/10 | 63.91 ± 8.85 | 25.17 ± 2.71 | 236.11 ± 29.05 |

The surface morphology of the sorafenib-coated polymer stents was observed using scanning electron microscopy. Figure 1A shows that unloaded and sorafenib-loaded PCL films have a smooth surface, indicating that drug may be evenly dispersed in the PCL polymer matrix. The yield of the polymer film was approximately 60% of the initial polymer content, and increased drug content did not significantly affect coating efficiency, as shown in Table 1. The higher sorafenib content did not significantly increase the thickness of the polymer film, but drug concentration per 1 cm$^2$ was dose-dependently increased. Table 2 shows the surface analysis of sorafenib-loaded polymer using X-ray photoelectron spectroscopy. Since PCL polymers have carbon, oxygen, and hydrogen atoms, the unloaded film (UF) revealed the existence of carbon and oxygen atoms. However, the sorafenib-loaded film (SF) showed fluoride, nitrogen, and sodium atoms since sorafenib has carbon, oxygen, hydrogen, fluoride, nitrogen, and sodium atoms (Table 2).

The drug-release behavior from SF was recorded, as shown in Figure 1B. Sorafenib was continuously released from the polymer film and films with lower drug content showed faster drug release than those with higher drug content. Figure 2 shows the degradation behavior of polymer films with and without sorafenib in vitro. The weight loss of the PCL was accelerated at 0.01 N NaOH

**Table 2** Surface analysis of sorafenib-incorporated PCL film using X-ray photoelectron spectroscopy

| XPS atomic % | | |
|---|---|---|
| **Atom** | **UF** | **SF** |
| C | 79.72 | 75.41 |
| F | ND | 0.42 |
| N | ND | 0.48 |
| Na | ND | 1.06 |
| O | 19.31 | 20.37 |
| S | ND | 0.51 |
| Si | 0.97 | 1.74 |

**Abbreviations:** PCL, poly(ε-caprolactone); UF, unloaded PCL film; SF, sorafenib-loaded PCL film; XPS, X-ray photoelectron spectroscopy; ND, no detection.

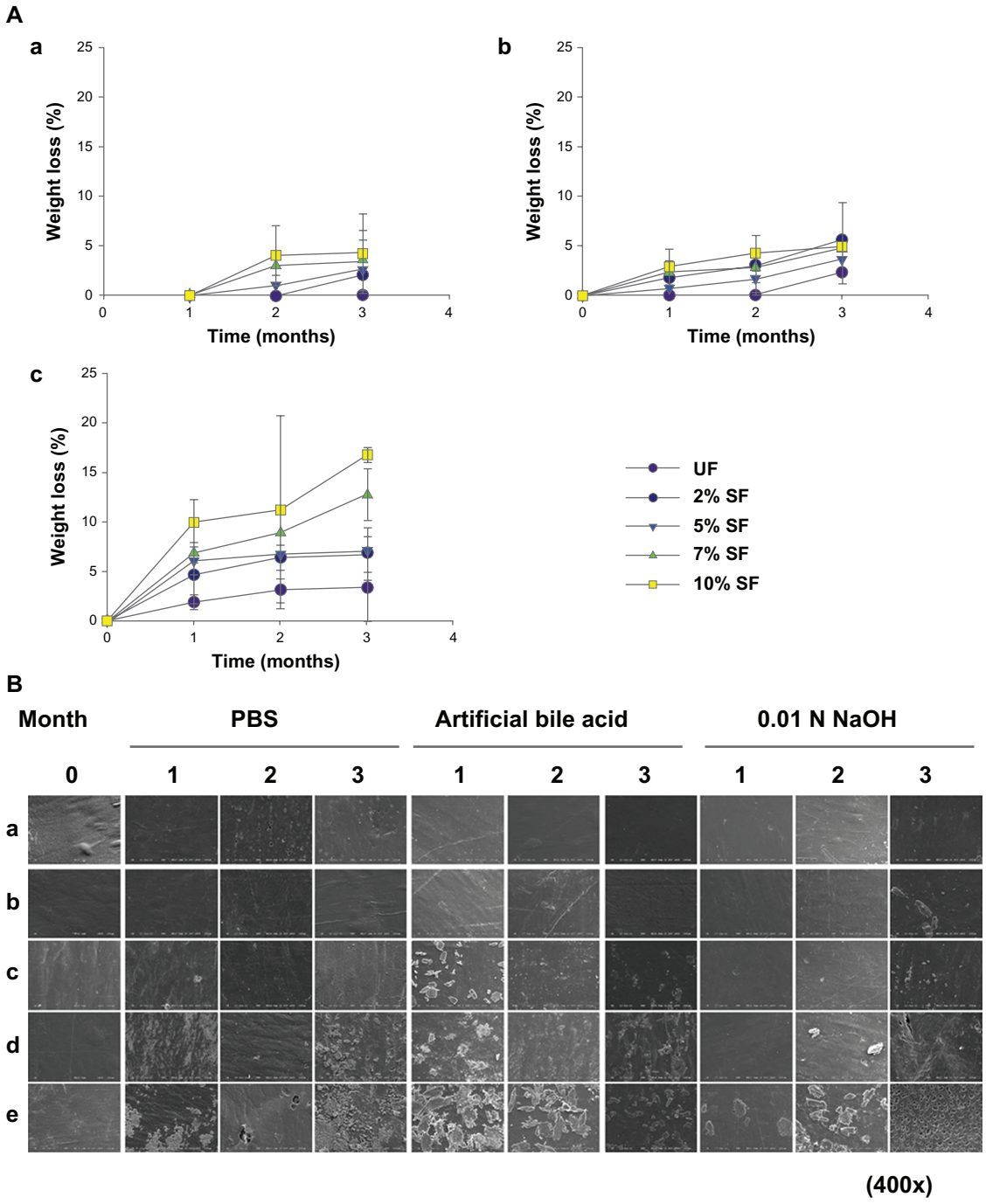


**Figure 2** (**A**) Degradation properties of sorafenib-loaded film. The weight loss of unloaded (UF) or sorafenib-loaded poly(ε-caprolactone) film (SF) was measured in the various media: phosphate-buffered saline (PBS) (**a**); artificial bile (**b**); 0.01 N NaOH (**c**). (**B**) Morphological observation of degradation of poly(ε-caprolactone) film in various media. (**a**) UF; (**b**) 2% (w/w) SF; (**c**) 5% (w/w) SF; (**d**) 7% (w/w) SF; (**e**) 10% (w/w) SF.

(Figure 2A(c)) rather than PBS (Figure 2A(a)) or artificial bile (Figure 2A(b)). In particular, the weight loss of SF was accelerated compared to UF, indicating that many pores can be generated on SF during drug release, and these pores may act as water channels to accelerate the degradation rate. These results indicated that drug-release kinetics may be principally controlled by polymer degradation rather than diffusion of drug molecules. Furthermore, the molecular weight of the PCL film was also recorded, as shown in Table 3. The molecular weight of PCL film rapidly decreased at 0.01 N NaOH and on SF. These results were also in accordance with the weight-loss results in Figure 2A. Figure 2B shows morphological changes of the polymer film. UF shows little change in surface morphology until 3 months in any incubation media. However, higher sorafenib content induced more serious changes in film-surface morphology.

**Table 3** Changes in molecular weight of PCL films

| Sample | Conditioned media | Time (months) | $M_w \times 10^{-4}$ | $M_n \times 10^{-4}$ | $M_w/M_n$ |
|---|---|---|---|---|---|
| UF | PBS | 0 | 19.21 | 14.83 | 1.30 |
| | | 1 | 19.29 | 14.65 | 1.32 |
| | | 2 | 19.13 | 14.28 | 1.34 |
| | | 3 | 14.32 | 7.24 | 1.98 |
| 10% SF | | 1 | 13.41 | 9.67 | 1.39 |
| | | 2 | 12.85 | 9.26 | 1.39 |
| | | 3 | 8.94 | 5.30 | 1.69 |
| UF | Artifical bile | 1 | 18.92 | 13.97 | 1.35 |
| | | 2 | 13.83 | 10.74 | 1.29 |
| | | 3 | 12.06 | 9.27 | 1.30 |
| 10% SF | | 1 | 10.90 | 8.29 | 1.31 |
| | | 2 | 7.47 | 5.52 | 1.35 |
| | | 3 | 6.32 | 4.46 | 1.42 |
| UF | 0.01 N NaOH | 1 | 18.57 | 13.73 | 1.35 |
| | | 2 | 17.86 | 13.60 | 1.31 |
| | | 3 | 12.67 | 6.30 | 2.01 |
| 10% SF | | 1 | 14.45 | 10.47 | 1.38 |
| | | 2 | 9.76 | 6.55 | 1.49 |
| | | 3 | 5.93 | 3.80 | 1.56 |

**Abbreviations:** PCL, poly(ε-caprolactone); $M_w$, weight average molecular weight; $M_n$, number average molecular weight; UF, unloaded PCL film; SF, sorafenib-loaded PCL film; PBS, phosphate-buffered saline.

More specifically, larger pores were generated at 10% (w/w) SF in 0.01 N NaOH media compared to others. These results support the results of Figure 2A and Table 3.

## Anticancer activity of sorafenib against HuCC-T1 cells in vitro

The anticancer activity of sorafenib was assessed by proliferation, invasion, and angiogenesis of HuCC-T1 cholangiocarcinoma cells in vitro, as shown in Figures 3–6. The viability of cancer cells was dose-dependently decreased, and half-maximal inhibitory concentration ($IC_{50}$) was 14.846 μg/mL (Figure 3A). The proliferation of cancer cells was completely inhibited at sorafenib doses greater than 25 μg/mL.

We tested the in vitro anticancer potential of SF on the assumption that the DES equipped with SF is installed in the bile duct and is in contact with the cancer site. First of all, we tested the effect of sorafenib contents of the polymer film on the proliferation of HuCC-T1 cholangiocarcinoma cells, as shown in Figure 3B–D. Cancer cells were seeded onto the polymer film and then allowed to proliferate. After 32 hours, they became full on UF surfaces, while the density of cancer cells was dose-dependently decreased on SF. In particular, the proliferation of cancer cells was completely inhibited at 10% (w/w) SF, indicating that proliferation of cancer cells was favorably inhibited by the release of sorafenib on the polymer film.

Figure 3C shows the effect of the absolute amount of released drug from the polymer film on the viability of HuCC-T1 cholangiocarcinoma cells. As shown in Figure 3C(a), the absolute amount of drug release continuously decreased according to the time course, and the drug remained in the polymer film was practically starved after 80 days of drug release. To evaluate the anticancer activity of the released drug, cell viability was recorded, as shown in Figure 3C(b). These experiments will enable us to assess the duration of the anticancer capacity of DESs equipped with SF in vivo. As shown in Figure 3C(b), the anticancer activity of the DES was properly maintained during drug release even though cell viability increased gradually. Furthermore, the DES loading 10% sorafenib showed higher anticancer activity than the others, indicating that growth inhibition of cancer cells responded to the release amount of sorafenib. Furthermore, apoptosis of cancer cells was studied using sorafenib and showed sorafenib was released from SF. Sorafenib at 50 mg/mL induced approximately 50% apoptosis and necrosis. The released sorafenib also properly induced apoptosis and necrosis, although the extent of these decreased according to the time course (Figure 2D). Media from UF did not significantly affect the apoptosis and necrosis of cancer cells.

## The effect of released sorafenib on the invasion, angiogenesis, and migration of cancer cells in vitro

The effect of SF on the invasion, angiogenesis, and migration of HuCC-T1 cells was assessed in vitro. To investigate the invasiveness of cancer cells, MMP-2 and Matrigel invasion assays were performed, as shown in Figure 4. MMP-2 secre-

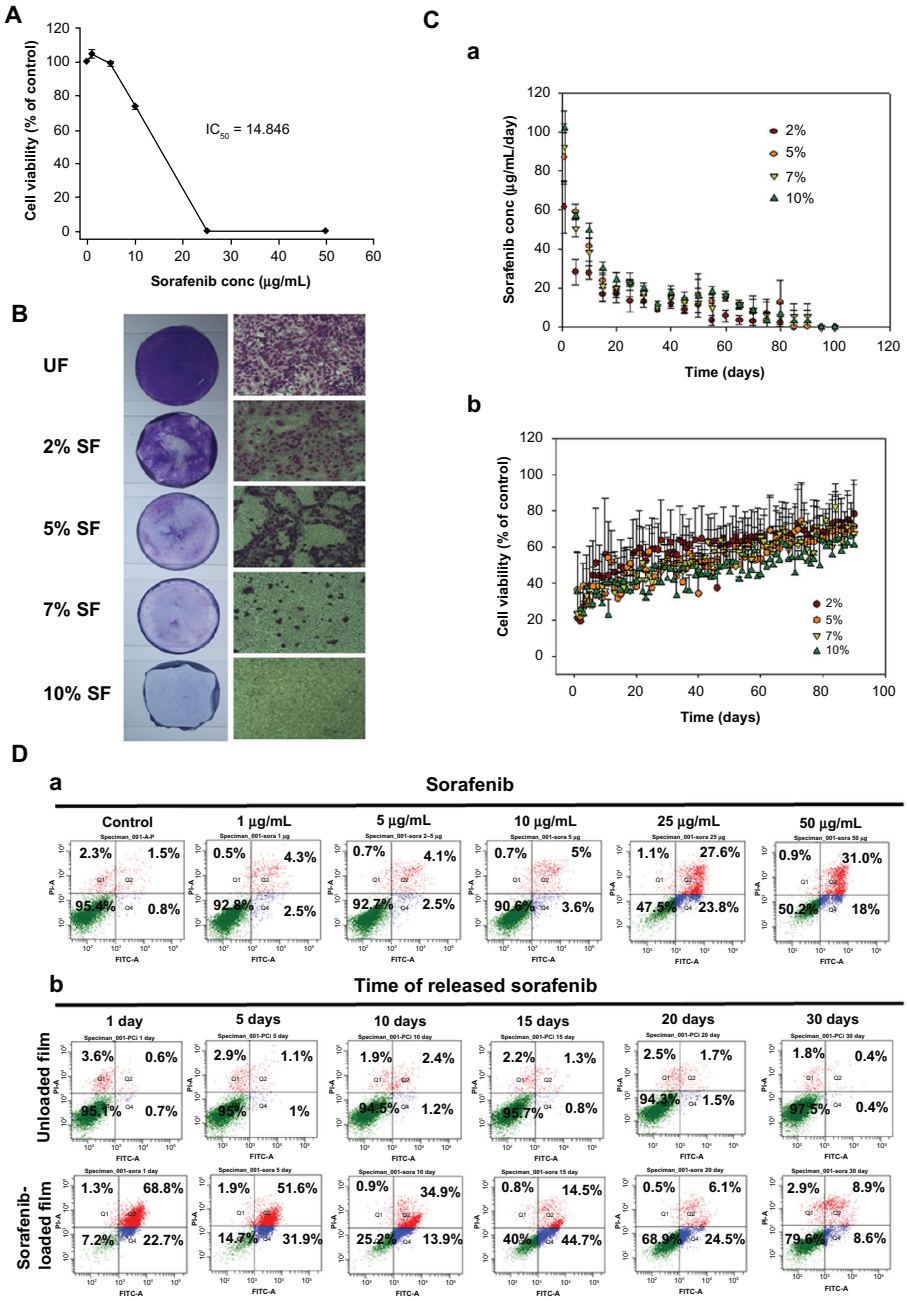


**Figure 3** (**A**) Effect of unloaded film (UF) or sorafenib-loaded film (SF) on the growth of HuCC-T1 cholangiocarcinoma cells. Cells ($2 \times 10^3$ cells/well in 96-well plate) were treated with DMSO (0.1% v/v, control) or indicated amounts of sorafenib for 32 hours. Cell growth was measured by MTT cell-proliferation assay. Values from three different experiments were expressed as means ± standard deviation (n = 3). (**B**) Comparison of HuCC-T1 cell proliferation on the sorafenib-loaded polymer film. $5 \times 10^5$ HuCC-T1 cells in RPMI 1640 media (FBS 10%) were seeded onto the PCL film; after 32 hours, H&E stained, 100×. (**C**) (**a**) The absolute amount of sorafenib released into the release media; (**b**) the effect of the released sorafenib from the sorafenib-loaded film on the viability of HuCC-T1 cholangiocarcinoma cells. (**D**) The effect of intact sorafenib (**a**) and sorafenib released from the sorafenib-loaded stent (**b**) on the apoptosis of HuCC-T1 cells.

tion from cancer cells was dose-dependently decreased by treatment with sorafenib (Figure 4A), and the invasiveness of cancer cells also dose-dependently decreased (Figure 4B). The invasiveness of cancer cells was completely inhibited at doses higher than 25 mg/mL of sorafenib. Interestingly, the invasion of cancer cells was inhibited by treatment of the released sorafenib from SF for the 30 days of the drug-release experiment (Figure 4B(d)), while UF did not significantly affect the invasiveness of cancer cells for the 30 days (Figure 4B(c)). These results indicate that the anti-invasive capacity of sorafenib can be maintained during its release from the polymer film. Figure 5 shows the effect of sorafenib and released sorafenib on the angiogenesis of cancer cells. To assess angiogenesis of cancer cells, conditioned media

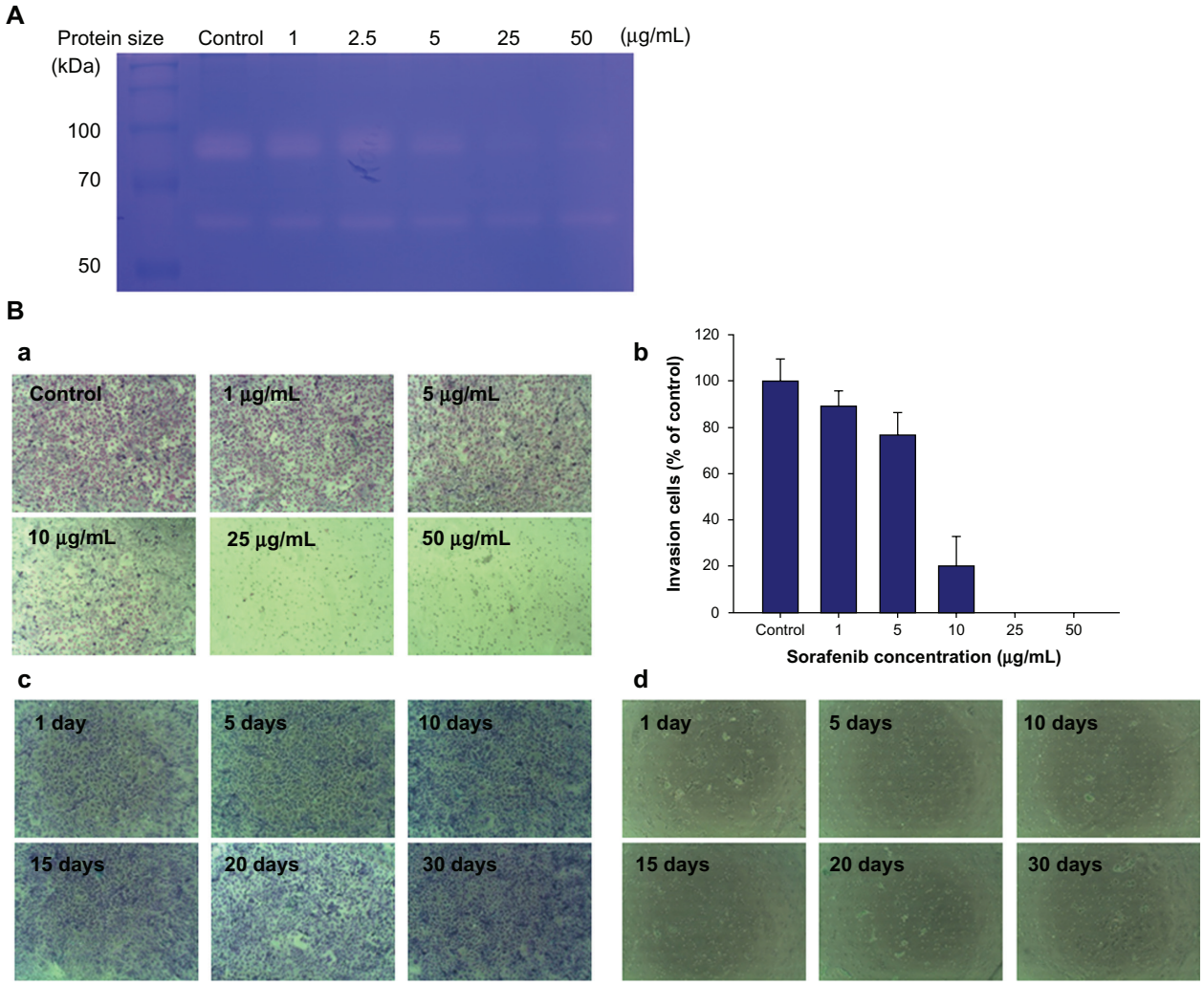


**Figure 4** (**A**) Effect of intact sorafenib or sorafenib released from the sorafenib-loaded film on the MMP-2/9 activity of HuCC-T1 cells. The cells were exposed to various concentrations of sorafenib for 32 hours, and then the conditioned media were used for gelatin zymography. (**B**) Effect of intact sorafenib (**a** and **b**), media taken from unloaded PCL film (**c**) and sorafenib released from the sorafenib-loaded film (**d**) on the invasion of HuCC-T1 cells. All groups H&E stained, 100×. Invasiveness of HuCC-T1 cells was assessed with Matrigel invasion assay. (**b**) The number of cells in four randomly selected microscopic fields per membrane was counted. $2 \times 10^4$ HuCC-T1 cells in the RPMI 1640 media (without FBS) were seeded onto the upper chamber, and the lower chamber was filled with RPMI 1640 media (with FBS 10%).

were prepared by treatment of cancer cells with sorafenib or released sorafenib from the polymer film, and these media were added to HUVECs in culture. The extent of angiogenesis of cancer cells was assessed by tube formation of HUVECs in the presence of conditioned media. HUVECs formed a network of capillary-like structures over 12 hours in the presence of conditioned media (Figure 5A, control). The length of tubes and the number of tube connections of HUVECs were decreased dose-dependently, and tube formation practically disappeared at more than 10 mg/mL sorafenib. Interestingly, the antiangiogenesis potential of sorafenib was maintained for 30 days, as shown in Figure 5B while UF did not significantly affect the formation of tubes by HUVECs. Figure 6 shows the effect of sorafenib and released sorafenib on the migration of cancer cells assessed by wound-healing assay. As shown in Figure 6A, the migration of cancer cells was inhibited by sorafenib treatment in a dose-dependent manner. Furthermore, the released sorafenib also inhibited the migration of cancer cells, and its antimigration activity was maintained for 30 days of drug release. These results indicate that intrinsic anticancer activity of sorafenib was maintained for the 30 days of the drug-release experiment.

## Antitumor activity of sorafenib stent in in vivo animal model

The anticancer activity of the SF in vivo was studied using an animal tumor xenograft model by subcutaneous injection of HuCC-T1 cells into the back of mice. When the size of the solid tumor reached 6 mm, SF and UF were implanted under the solid tumor mass, as shown in Figure 7. Tumor

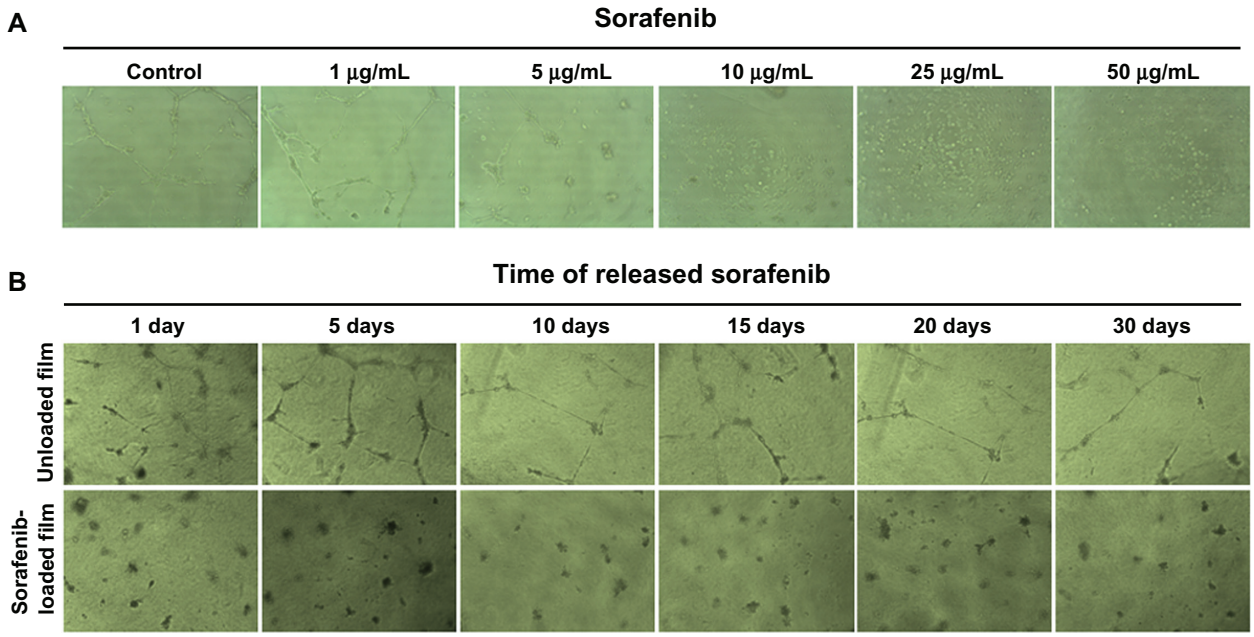


**Figure 5** Effect of intact sorafenib (**A**) or sorafenib released from sorafenib-loaded film (**B**) on the angiogenesis of HuCC-T1 cholangiocarcinoma cells in vitro.
**Notes:** Conditioned media were from cancer cell culture with treatment of sorafenib. Conditioned media were added to a HUVECs culture plate. The length of tubes and the number of tube connections were evaluated by comparison with 0 μM of sorafenib concentration. All images were observed with microscopy (100×).

volume increased gradually (Figure 7C, control), and body weight slightly increased (Figure 7D, control). When SF was implanted under the solid tumor, the growth of tumor volume was properly inhibited, and the body weight of the mouse did not significantly change. Interestingly, UF also affected the growth of tumor mass. This finding may be due to dissected blood vessels during the implantation procedure, which might have caused reduced supply of blood or nutrients. Tumor mass treated with SF was smaller than that of UF, indicating that SF has antitumor activity against the animal tumor xenograft model. Since sorafenib has lower intrinsic cytotoxicity compared to common anticancer agents, such as doxorubicin and cisplatin, suppression of tumor growth may be due to inhibition of molecular signals, such as

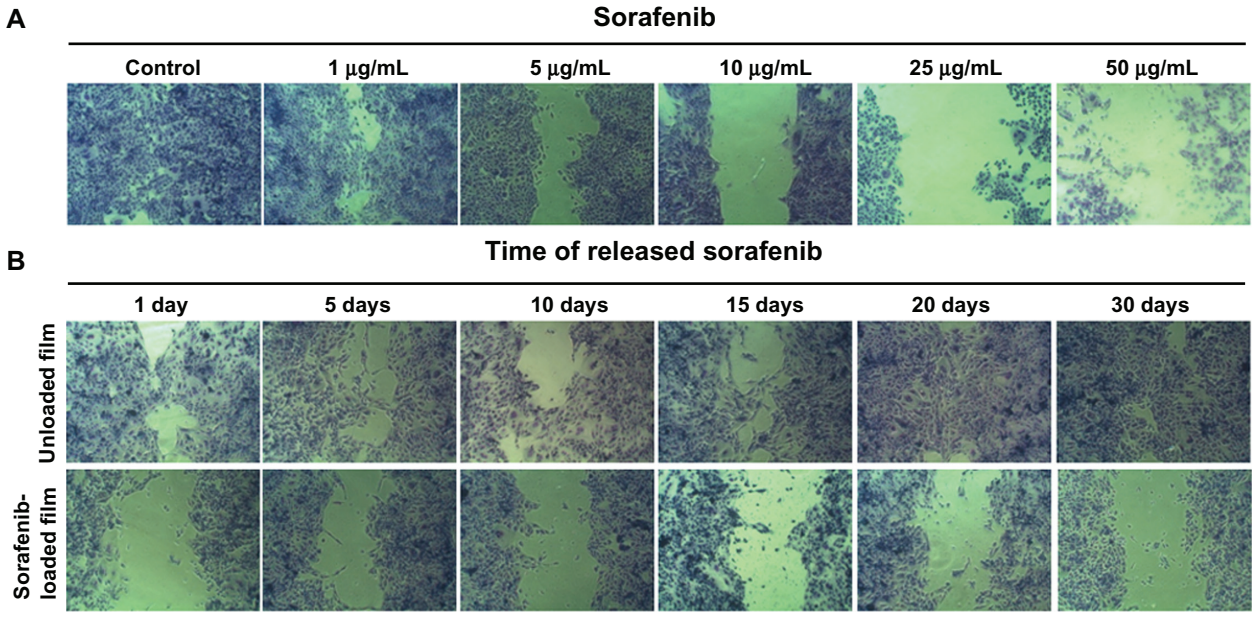


**Figure 6** Effect of intact sorafenib (**A**) or sorafenib released from sorafenib-loaded stent (**B**) on the migration potential of HuCC-T1 cholangiocarcinoma cells in vitro.
**Note:** All groups H&E stained, 100×.

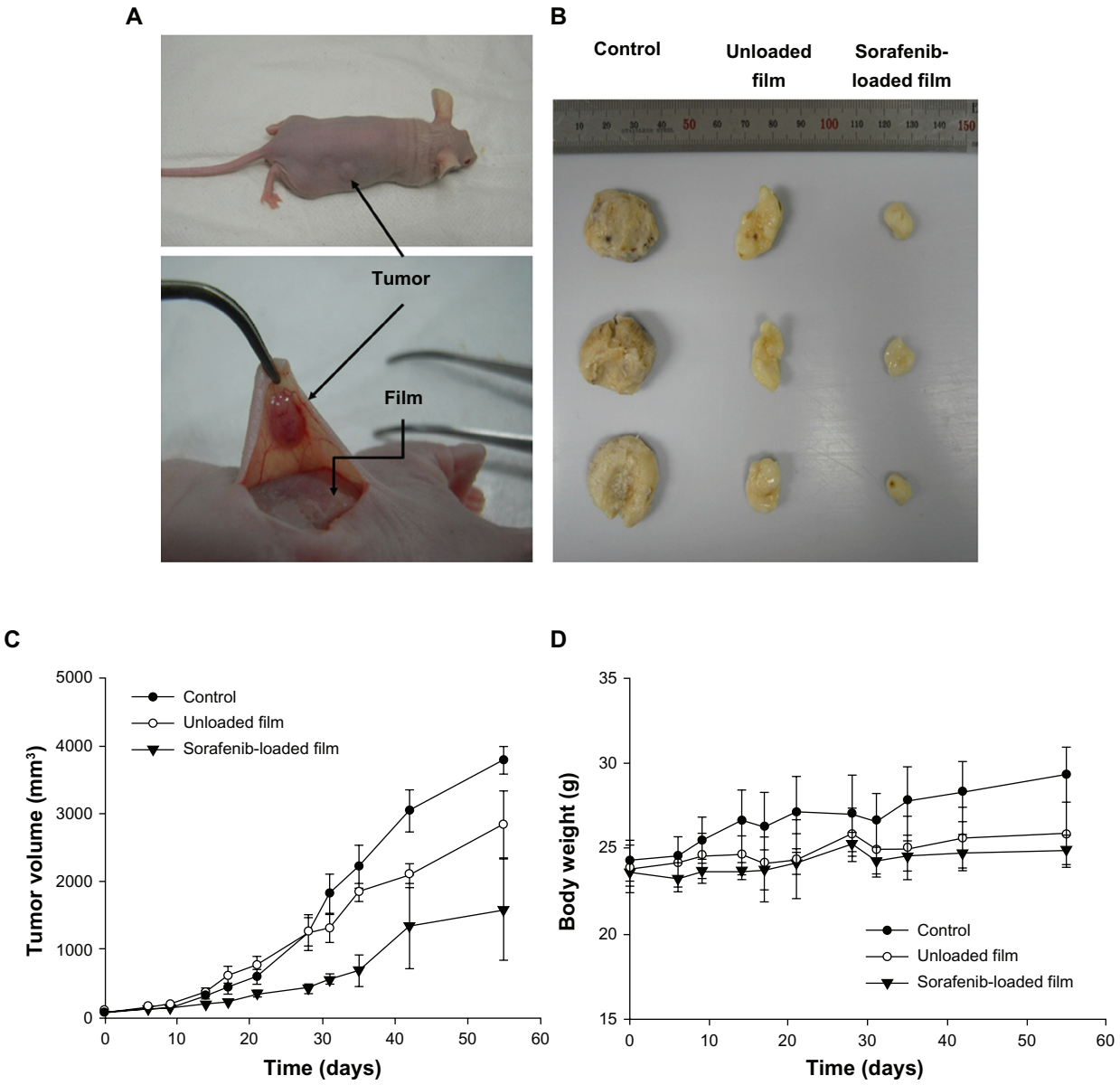


**Figure 7** (**A**–**D**) Antitumor activity of sorafenib-loaded poly(ε-caprolactone) (PCL) film.
**Notes:** (**A**) Sorafenib-loaded film was implanted under the tumor mass; (**B**) tumor mass from mice 43 days after tumor implantation; (**C**) changes in tumor weight; (**D**) changes in body weight.

apoptosis-related protein, mitosis-related protein, and MMP. As shown in Figure 8, apoptosis signals such as terminal deoxynucleotidyl transferase deoxyuridine-triphosphate nick-end labeling staining, Bcl-2-associated death promoter, caspase-3, and cleaved caspase-3 were clearly induced by treatment of SF. Figure 9A shows the effect of SF on the expression of MMP-9. As shown in Figure 9a, the expression of MMP-9 evidently decreased after treatment with SF. Furthermore, the expression of Bcl-2 and Bcl-x was decreased. The expression of mitosis-related proteins such as pan-janus kinase/stress-activated protein kinase 1 also decreased (Figure 9C). STAT5 and ERK signaling is associated with proliferation of cancer cells. The expression of STAT5 and ERK significantly decreased with SF (Figures 9C and 10). Since protein expression with treatment of UF was similar to control, UF did not affect the molecular aspect of the tumor. Furthermore, these results indicated that SF has strong anti-tumor activity in the in vivo mouse tumor xenograft model.

## Discussion

The incidence and the mortality rate of cholangiocarcinoma, a malignant tumor arising from the epithelium of the bile ducts, are increasing worldwide.[21–24] Since early diagnosis of cholangiocarcinoma is difficult, many patients are diagnosed

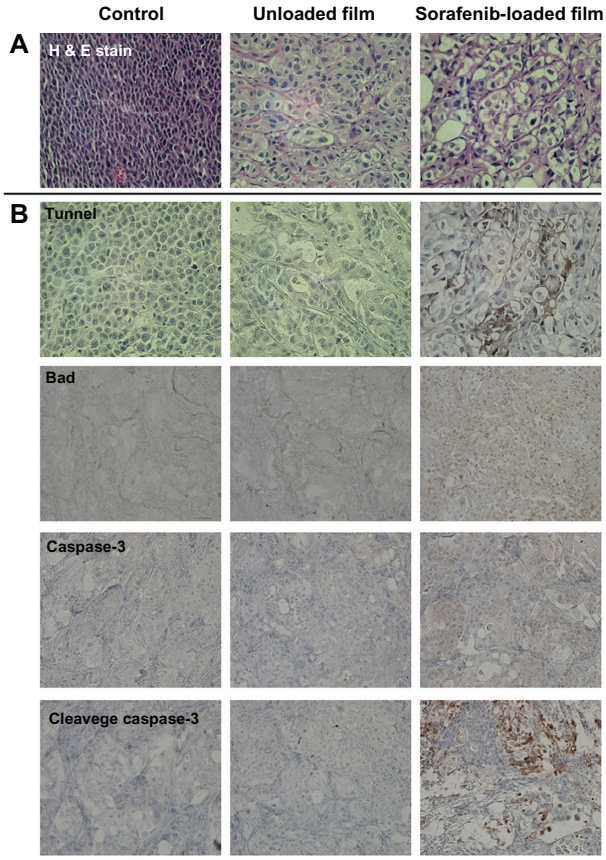


**Figure 8** (**A** and **B**) Immunohistochemical analysis.
**Notes:** (**A**) H&E staining; (**B**) tunnel staining, Bad, caspase-3, and cleaved caspase-3 staining.

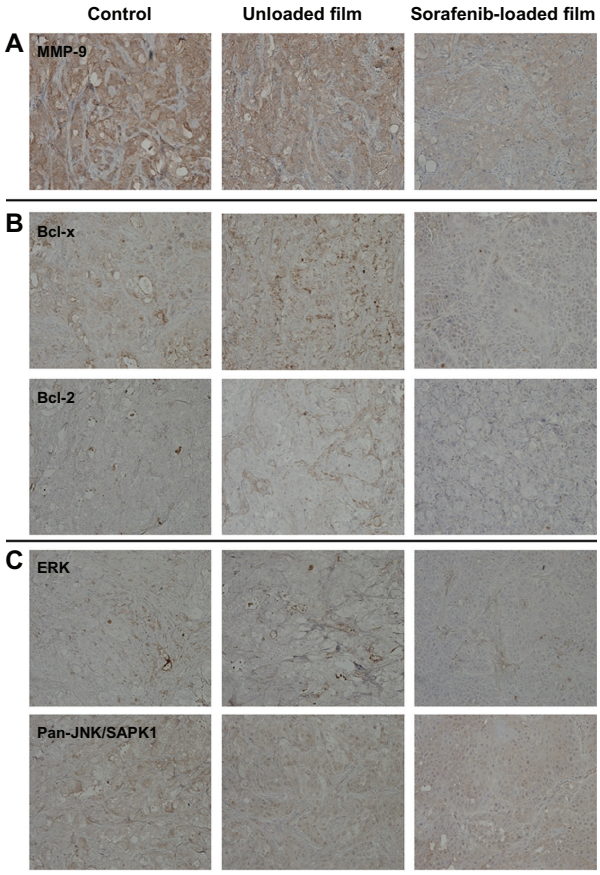


**Figure 9** (**A**–**C**) Immunohistochemical analysis.
**Notes:** (**A**) MMP-9; (**B**) Bcl-x and Bcl-2; (**C**) ERK and pan-JNK/SAPK 1.

in an advanced state. Surgical extirpation is regarded as the ideal choice for long-term survival of patients. Furthermore, the recurrence rate is quite high even with complete surgical resection. Surgical resection of the tumor from these patients is often not feasible, due to the anatomical location of the cancer and the presence of extra- or intrahepatic metastases.[23] Furthermore, conventional therapy, such as radiation therapy and chemotherapy, is not feasible. Since early invasion or metastasis of cholangiocarcinoma is a distinguished feature from other types of cancer,[21–24] local treatment using DESs is regarded as a promising candidate for improving palliation and survival of patients with unresectable cholangiocarcinoma.[23,25] Mezawa et al[25] reported that carboplatin-coated tubes showed an antitumor effect against subcutaneous tumors inoculated in nude mice, and they observed a 60% efficacy rate in patients with unresectable cholangiocarcinoma.

Sorafenib, a small-molecular inhibitor of several tyrosine protein kinases,[12] is known to inhibit tumor progression and angiogenesis. Sugiyama et al[17] reported that sorafenib is effective in inhibiting the phosphorylation of MEK and mitogen-activated protein kinase, as well as the interleukin-6-induced phosphorylation of STAT3. They showed that oral administration of sorafenib was effective in inhibiting tumor growth and decreasing microvessel density in an animal xenograft tumor model of cholangiocarcinoma. Even though sorafenib was shown to have low activity against advanced biliary tract carcinoma in phase II clinical trials, it is regarded as having therapeutic benefit for patients.[26] Other clinical trials have also emphasized the therapeutic benefit against metastatic gallbladder carcinoma and cholangiocarcinoma.[27] We previously reported that sorafenib was tolerable for most patients in clinical practice and in therapeutic progression during sorafenib therapy.[28] Other kinds of anticancer drugs such as gemcitabine and cisplatin were also tried clinically for the treatment of biliary tract cancer.[7–9] However, Xinopoulos et al reported that gemcitabine therapy combined with a metallic stent for patients with advanced pancreatic cancer failed to improve survivability and quality of life.[29] Even though the safety of a gemcitabine-eluting stent against the biliary tract in a porcine model was reported, the clinical efficacy of gemcitabine plus stenting is still questionable.[30]

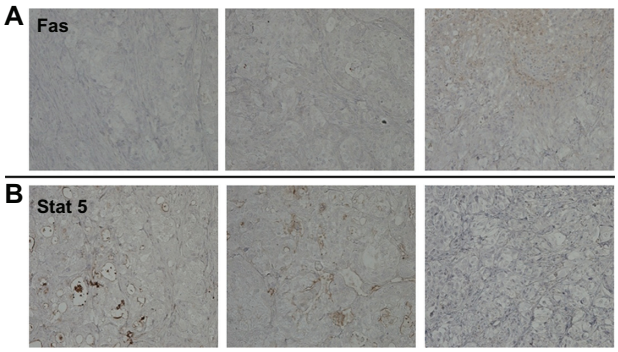


**Figure 10** Immunohistochemical analysis. (**A**) Fas; (**B**) STAT5.

Selection of a controlled drug-delivery technology suitable for each drug depends on many factors, including physicochemical properties of the drug, duration of release, and release profile.[31] Localized delivery of a drug directly to the target site results in the prevention of restenosis, without the side effects associated with systemic delivery of the same drug at higher concentrations.[31] The aim of localized drug delivery using a DES is to inhibit the growth and migration of cholangiocarcinoma cells, as well as prevention of inflammatory responses.[32] The DES approach for the local treatment of tumors has several advantages, ie, biologically active agents can be directly delivered to the target site, resulting in therapeutically effective drug concentrations in the local tissue, with minimal systemic release of the drug, and thus negligible risk of systemic toxicity.[33] To confirm the anticancer activity of SF, HuCC-T1 cells were seeded onto the films, as shown in Figure 3B. The PCL film itself did not significantly affect the proliferation and migration of cancer cells, ie, cancer cells were closely packed on the film surfaces after 32 hours of culture. However, the density of cancer cells decreased dose-dependently on SF, indicating that growth of HuCC-T1 cells was properly inhibited on SF, while UF (Figure 3B) did not affect the growth of cancer cells. Because degradation of the polymer film was very slow (Figure 1C and D, only 5% weight loss for 3 months), SF coated onto a metal stent may inhibit stent ingrowth and clogging of tumor cells. Furthermore, our results showed that sorafenib itself effectively inhibited the growth of cancer cells in vitro, with an $IC_{50}$ of 14.846 mg/mL (Figure 3A). Our $IC_{50}$ value was slightly higher than the results of other reports,[12] and this difference may be due to the difference in experimental conditions. Even though sorafenib concentration higher than 10 mg/mL was effective in inhibiting the proliferation of cancer cells (Figure 3A), apoptosis of cancer cells clearly increased at concentrations higher than 25 mg/mL (Figure 3D). Huether et al[18] also reported that sorafenib alone or in combination with other anticancer drugs potently suppressed the growth of human cholangiocarcinoma cells. Because body weight was not significantly affected by treatment with SF, SF may have negligible inherent toxicity, indicating that suppression of tumor growth may be due to the apoptosis of tumor cells and suppression of molecular signals. Figures 8–10 demonstrate the suppression of various molecular signals in the tumor mass.

Since MMP is an important enzyme for the degradation of basement membranes during tumor invasion, expression of MMP is regarded as an indicator of poor prognosis.[34–37] Our results showed that sorafenib was effective in decreasing MMP-9 expression in HuCC-T1 cells in vitro and in vivo.

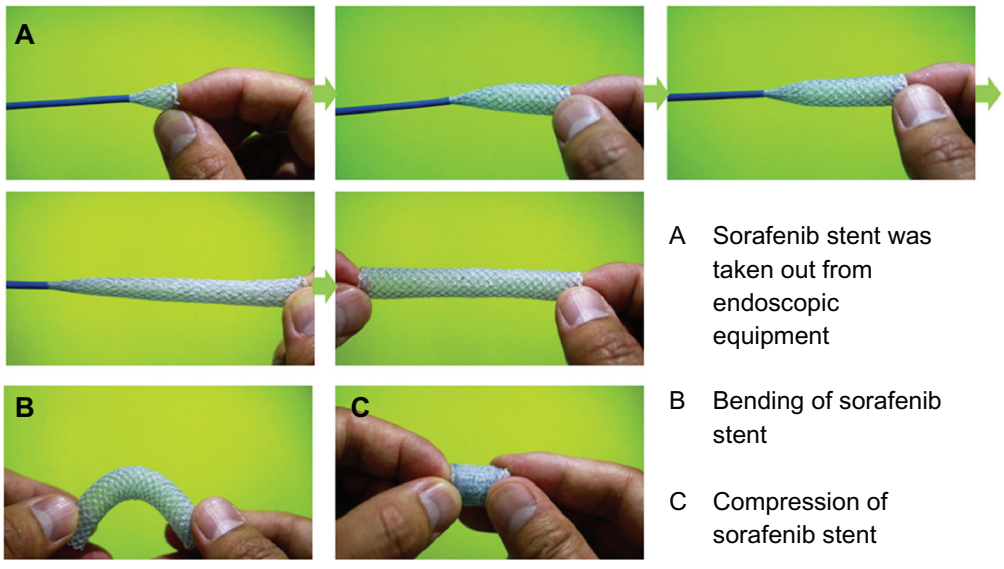


**Figure 11** The sorafenib-loaded stent being taken out from the endoscopic equipment.

Furthermore, the Matrigel assay demonstrated the anti-invasive effect of sorafenib in cholangiocarcinoma cells (Figure 4). This finding was also demonstrated by the invasion test of cancer cells, ie, invasion of HuCC-T1 cells was inhibited by treatment with sorafenib, and the released sorafenib from the PCL film also effectively inhibited invasion of cancer cells even at 30 days. In particular, invasion of cancer cells or tube formation of HUVECs significantly decreased when sorafenib concentrations were greater than 10 mg/mL. We also found that sorafenib is effective in inhibiting tube formation of HUVECs in a dose-dependent manner (Figure 5). Our results demonstrated that the released sorafenib from the PCL films as well as intact sorafenib maintained antiangiogenesis activities against tube formation of HUVECs, even after 30 days of the drug-release experiment, while UF did not have any effect on the results. Furthermore, the migration of tumor cells was effectively inhibited by the released sorafenib as well as intact sorafenib, as shown in Figure 6. Since the metastatic invasion and angiogenesis potential of cholangiocarcinoma cells are regarded as causes of poor prognosis after chemotherapy or radiotherapy, inhibition of these factors in vitro may enhance the therapeutic potential of sorafenib-eluting stents. Practically, SF significantly inhibited the growth of the tumor in the mouse tumor xenograft model, as shown in Figure 7. As shown in Figures 8–10, the signals show apoptosis or suppression of proliferation of tumor cells by SF, while UF was not significantly different to control. MMP-9 was also significantly suppressed by treatment with SF.

Furthermore, a defect or crack on the polymer film surface is known to affect the potential of DESs. Therefore, we tested the SF-coated metal stent with endoscopic equipment by the insertion and exfiltration method of DESs, as shown in Figure 11. The polymer films did not show distinct defects or cracks on the surface of the polymer film with repeated insertion and exfiltration.

Our results show that SF as a DES material is a promising candidate for the treatment of cholangiocarcinoma.

## Conclusion

We described the preparation of SF and its anticancer activity against HuCC-T1 cells. Sorafenib inhibited the proliferation of cancer cells in a dose-dependent manner, and its $IC_{50}$ was approximately 10 μM. Furthermore, sorafenib was effective in suppressing MMP-2 expression and invasion of tumor cells, as well as tube formation of HUVECs. We demonstrated that SF has equivalent anticancer activity against in vitro cell culture and in vivo animal tumor xenograft model compared to sorafenib itself. We suggest that SF and its DES is a promising candidate for the treatment of cholangiocarcinoma.

## Acknowledgments

This study was supported by a grant of the Korean Healthcare Technology R&D Project, Ministry of Health and Welfare, South Korea (project A091047).

## Disclosure

The authors report no conflicts of interest in this work.

## References

1. Leelawat K, Narong S, Udomchaiprasertkul W, Leelawat S, Tungpradubkul S. Inhibition of PI3K increases oxaliplatin sensitivity in cholangiocarcinoma cells. *Cancer Cell Int*. 2009;9:3.
2. Nakajima T, Kondo Y, Miyazaki M, Okui K. A histopathologic study of 102 cases of intrahepatic cholangiocarcinoma: histologic classification and modes of spreading. *Hum Pathol*. 1988;19(10):1228–1234.
3. Olnes MJ, Erlich R. A review and update on cholangiocarcinoma. *Oncology*. 2004;66(3):167–179.
4. Scheithauer W. Review of gemcitabine in biliary tract carcinoma. *Semin Oncol*. 2002;29(6 Suppl 20):40–45.
5. Cereda S, Passoni P, Reni M, et al. The cisplatin, epirubicin, 5-fluorouracil, gemcitabine (PEFG) regimen in advanced biliary tract adenocarcinoma. *Cancer*. 2010;116(9):2208–2214.
6. Hong YS, Lee J, Lee SC, et al. Phase II study of capecitabine and cisplatin in previously untreated advanced biliary tract cancer. *Cancer Chemother Pharmacol*. 2007;60(3):321–328.
7. Kim ST, Park JO, Lee J, et al. A phase II study of gemcitabine and cisplatin in advanced biliary tract cancer. *Cancer*. 2006;106(6):1339–1346.
8. Valle J, Wasan H, Palmer DH, et al. Cisplatin plus gemcitabine versus gemcitabine for biliary tract cancer. *N Engl J Med*. 2010;362(14):1273–1281.
9. Valle JW, Wasan H, Johnson P, et al. Gemcitabine alone or in combination with cisplatin in patients with advanced or metastatic cholangiocarcinomas or other biliary tract tumours: a multicentre randomised phase II study – the UK ABC-01 Study. *Br J Cancer*. 2009;101(4):621–627.
10. Park SW, Lee DH, Park YS, Chung JB, Kang JK, Song SY. Percutaneous transhepatic choledochoscopic injection of ethanol with OK-432 mixture for palliation of malignant biliary obstruction. *Gastrointest Endosc*. 2003;57(6):769–773.
11. Lee DH. [Drug-eluting stent in gastrointestinal disease.] *Korean J Gastroenterol*. 2007;49(5):294–299. Korean.
12. Wilhelm SM, Adnane L, Newell P, Villanueva A, Llovet JM, Lynch M. Preclinical overview of sorafenib, a multikinase inhibitor that targets both Raf and VEGF and PDGF receptor tyrosine kinase signaling. *Mol Cancer Ther*. 2008;7(10):3129–3140.
13. Liu L, Cao Y, Chen C, et al. Sorafenib blocks the RAF/MEK/ERK pathway, inhibits tumor angiogenesis, and induces tumor cell apoptosis in hepatocellular carcinoma model PLC/PRF/5. *Cancer Res*. 2006; 66(24):11851–11858.
14. Qun W, Tao Y. Effective treatment of advanced cholangiocarcinoma by hepatic arterial infusion chemotherapy combination with sorafenib: one case report from China. *Hepatogastroenterology*. 2010; 57(99–100):426–429.
15. LaRocca RV, Hicks MD, Mull L, Foreman B. Effective palliation of advanced cholangiocarcinoma with sorafenib: a two-patient case report. *J Gastrointest Cancer*. 2007;38(2–4):154–156.
16. Wiedmann MW, Mossner J. Molecular targeted therapy of biliary tract cancer – results of the first clinical studies. *Curr Drug Targets*. 2010;11(7):834–850.
17. Sugiyama H, Onuki K, Ishige K, et al. Potent in vitro and in vivo antitumor activity of sorafenib against human intrahepatic cholangiocarcinoma cells. *J Gastroenterol*. 2011;46(6):779–789.

18. Huether A, Hopfner M, Baradari V, Schuppan D, Scherubl H. Sorafenib alone or as combination therapy for growth control of cholangiocarcinoma. *Biochem Pharmacol*. 2007;73(9):1308–1317.
19. Jin SG, Jeong YI, Jung S, Ryu HH, Jin YH, Kim IY. The effect of hyaluronic acid on the invasiveness of malignant glioma cells: comparison of invasion potential at hyaluronic acid hydrogel and matrigel. *J Korean Neurosurg Soc*. 2009;46(5):472–478.
20. Okabe H, Beppu T, Hayashi H, et al. Hepatic stellate cells accelerate the malignant behavior of cholangiocarcinoma cells. *Ann Surg Oncol*. 2011;18(4):1175–1184.
21. Lim JH. Cholangiocarcinoma: morphologic classification according to growth pattern and imaging findings. *AJR Am J Roentgenol*. 2003; 181(3):819–827.
22. Shen FZ, Zhang BY, Feng YJ, et al. Current research in perineural invasion of cholangiocarcinoma. *J Exp Clin Cancer Res*. 2010; 29:24.
23. Gores GJ. Cholangiocarcinoma: preventing invasion as anti-cancer strategy. *J Hepatol*. 2003;38(5):671–673.
24. Sirica AE. Cholangiocarcinoma: molecular targeting strategies for chemoprevention and therapy. *Hepatology*. 2005;41(1):5–15.
25. Mezawa S, Homma H, Sato T, et al. A study of carboplatin-coated tube for the unresectable cholangiocarcinoma. *Hepatology*. 2000;32(5): 916–923.
26. Bengala C, Bertolini F, Malavasi N, et al. Sorafenib in patients with advanced biliary tract carcinoma: a phase II trial. *Br J Cancer*. 2010; 102(1):68–72.
27. El-Khoueiry AB, Rankin CJ, Ben-Josef E, et al. SWOG 0514: a phase II study of sorafenib in patients with unresectable or metastatic gallbladder carcinoma and cholangiocarcinoma. *Invest New Drugs*. 2012;30(4):1646–1651.
28. Woo HY, Heo J, Yoon KT, et al. Clinical course of sorafenib treatment in patients with hepatocellular carcinoma. *Scand J Gastroenterol*. 2012;47(7):809–819.
29. Xinopoulos D, Dimitroulopoulos D, Karanikas I, et al. Gemcitabine as palliative treatment in patients with unresectable pancreatic cancer previously treated with placement of a covered metal stent. A randomized controlled trial. *J BUON*. 2008;13(3):341–347.
30. Chung MJ, Kim H, Kim KS, Park S, Chung JB, Park SW. Safety evaluation of self-expanding metallic biliary stents eluting gemcitabine in a porcine model. *J Gastroenterol Hepatol*. 2012;27(2):261–267.
31. Acharya G, Park K. Mechanisms of controlled drug release from drug-eluting stents. *Adv Drug Deliv Rev*. 2006;58(3):387–401.
32. Smith EJ, Rothman MT. Antiproliferative coatings for the treatment of coronary heart disease: what are the targets and which are the tools? *J Interv Cardiol*. 2003;16(6):475–483.
33. McLean DR, Eiger NL. Stent design: implications for restenosis. *Rev Cardiovasc Med*. 2002;3 Suppl 5:S16–S22.
34. Terada T, Okada Y, Nakanuma Y. Expression of immunoreactive matrix metalloproteinases and tissue inhibitors of matrix metalloproteinases in human normal livers and primary liver tumors. *Hepatology*. 1996;23(6):1341–1344.
35. Miwa S, Miyagawa S, Soeda J, Kawasaki S. Matrix metalloproteinase-7 expression and biologic aggressiveness of cholangiocellular carcinoma. *Cancer*. 2002;94(2):428–434.
36. Subimerb C, Pinlaor S, Khuntikeo N, et al. Tissue invasive macrophage density is correlated with prognosis in cholangiocarcinoma. *Mol Med Rep*. 2010;3(4):597–605.
37. Kirimlioğlu H, Türkmen I, Başsüllü N, Dirican A, Karadağ N, Kirimlioğlu V. The expression of matrix metalloproteinases in intrahepatic cholangiocarcinoma, hilar (Klatskin tumor), middle and distal extrahepatic cholangiocarcinoma, gallbladder cancer, and ampullary carcinoma: role of matrix metalloproteinases in tumor progression and prognosis. *Turk J Gastroenterol*. 2009;20(1):41–47.